FED-Vol. 5

Advances in Grid Generation

presented at

APPLIED MECHANICS, BIOENGINEERING, AND
FLUIDS ENGINEERING CONFERENCE
HOUSTON, TEXAS
JUNE 20-22, 1983

sponsored by

THE FLUIDS ENGINEERING DIVISION, ASME

edited by

KIRTI N. GHIA
URMILA GHIA
UNIVERSITY OF CINCINNATI

THE AMERICAN SOCIETY OF MECHANICAL ENGINEERS
United Engineering Center 345 East 47th Street New York, N. Y. 10017

EFFICIENT TURBOMACHINERY GRID GENERATION USING TRAUPEL'S CONFORMAL MAPPING

Stephen R. Kennon
Undergraduate Research Assistant
Department of Aerospace Engineering
and Engineering Mechanics
University of Texas at Austin
Austin, Texas 78712

George S. Dulikravich
Assistant Professor
Associate Member ASME
Department of Aerospace Engineering
and Engineering Mechanics
University of Texas at Austin
Austin, Texas 78712

ABSTRACT

A fast computer code is developed that generates up to four sequentially refined boundary-fitted quasi-orthogonal three-dimensional periodic computational O-type grids applicable to axial turbomachinary flow field calculations. The grid generating technique is based on a sequence of conformal mappings and non-orthogonal coordinate stretching and shearing transformations. A periodic strip of the cascade flow field is mapped conformally onto a deformed oval using the analytic mapping functions developed by Traupel, and one bilinear transformation, the entire sequence being explicit and analytically invertible. The final step of opening the deformed oval into a near rectangle is performed using simple polar coordinates. The near rectangle is transformed to an exact rectangle using nonorthogonal stretching and shearing. This sequence does not require iterative inversion of the mapping functions. It also avoids conformal mapping onto an exact circle that involves use of the Fourier transforms. Consequently, the present grid generation technique is considerably faster than other known techniques, and is applicable to both compressor and turbine realistically shaped cascade geometries. In particular, this technique can generate three-dimensional grids for very thick, closely spaced, highly cambered and highly staggered turbine rotors or stators.

NOMENCLATURE

A'	Amplitude of sine function in the "strip" plane interior grid generation scheme
A,B,C	Bilinear mapping function constants
β	Local stagger angle, radians
$\Delta\tau$	Enclosed angle at the leading or trailing edge
i	Complex number $i = \sqrt{-1}$
R_{AV}	Average radius of airfoil contour in Z4-plane
$r_h(x)$	Radius of the hub
$r_s(x)$	Radius of the shroud or duct
z_K	Kth complex plane in the forward conformal mapping sequence ($z_K = X_K + iY_K$), $K = 1,2,\ldots,6$
z_{KS}	z_K-plane singularity, $K = 1,2,\ldots,6$

Subscripts

LE	Leading edge
P	Downstream infinity
TE	Trailing edge
w	Wake

INTRODUCTION

Computational grids for numerical analysis and design of turbomachinery flow fields usually have to satisfy a geometric periodicity condition. At the same time it is desirable that one of the grid lines follows the approximate shape of the wake. If grids are to be regenerated during the iterative flow calculation so that the regions of particular interest (for example, shock waves, vortex sheets, etc.) can be better resolved, the regeneration process should be as fast as possible.

Presently, there are three basic methods for generating boundary-fitted computational grids for turbomachinery flow field computations. The most traditional and the least expensive is the simple non-orthogonal shearing of the coordinate line in the periodicity (cascade) direction. Such grids suffer from an excessive nonorthogonality (1). The second technique is based on the solution of Poisson's equations thus representing the most costly approach (2). The third technique is based on a sequence of conformal mappings (3,4). This technique offers the best combination of low cost/high quality cascade grids, because

it utilizes analytic functions, most of which are also analytically invertible. If it is desired that the two families of grid lines be mutually orthogonal, a certain form of Theodorsen-Garrick complex exponential series technique and elliptic integrals must be used (5). Nevertheless, most of the present numerical techniques for the integration of the flow governing equations do not require strict grid orthogonality. Hence, simple coordinate stretching and nonorthogonal shearing can be used thus significantly reducing the computer time required for grid generation (5,6,7,8).

The first in a sequence of conformal mappings is usually an analytic function that maps the exterior of a simple contour onto a circular or oval shaped domain. The original contours can be a cascade of straight slits of finite length and zero thickness (4,6) or a cascade of semi-infinite straight slits having zero thickness (7,8). Both approaches are useful for generating grids applicable to axial compressor cascades, but fail for highly cambered, thick, closely spaced and highly staggered axial turbine cascades. Besides, in both cases the main mapping function must be inverted iteratively for any non-zero stagger angle. This part of the grid generation procedure consumes most of the computer time. A somewhat more flexible first mapping is the ratio of sine functions (3,9) although this function must also be inverted iteratively.

In three-dimensional problems the blades have arbitrary spanwise distributions of taper, sweep, dihedral, and twist angles. The local airfoil shapes can vary in an arbitrary fashion along the blade span. The rotor hub and the duct (or shroud) can have different axisymmetric shapes. Such an arbitrary three-dimensional physical domain is first discretized in the spanwise direction by a number of coaxial axisymmetric surfaces (Fig. 1). Each of these surfaces is then discretized using two-dimensional grid generation. A simple technique for converting a fully three-dimensional problem into a sequence of two-dimensional problems is explained in reference (6). Since this grid generating technique is very fast, a minimal additional amount of computer time is required for mapping the flow field boundaries along with the airfoil contour from the physical plane to the computational plane. These boundaries can be arbitrarily prescribed by the user. For cascade flow analyses, the boundaries must be periodic in the cascade direction (Fig. 2). Hence, points along the periodic boundaries are redistributed evenly along the boundary arc-length coordinate using cubic spline fitting and interpolation. The points may also be clustered closer to the airfoil (away from upstream and downstream infinities) by a simple sine stretching function. Once the boundary points have been determined, the grid is generated by the following sequence of mappings and re-mappings.

1. Traupel's Conformal Transformation

The problems of additional computer time requirement for the iterative inversion of a mapping function and inadequate flexibility of certain mapping functions can be overcome with Traupel's conformal transformation (10,11)

$$Z_2 = \coth(Z_1 - Z_{1S}) \tag{1}$$

The Z_1 (physical) complex plane singularity, Z_{1S}, should be positioned inside the airfoil contour, near the leading edge for negative stagger angles and near the trailing edge for positive stagger angles.

This complex variable function conformally maps the outside of an airfoil, including the boundaries, onto the inside of an irregularly shaped contour (Fig. 3). Upstream ($-\infty$) and downstream ($+\infty$) infinity map into the singular points $Z_2 = -1$ and $Z_2 = +1$, respectively. Note that the inverse of this mapping function is analytically obtainable:

$$Z_1 = \ln\left(\frac{Z_2 + 1}{Z_2 - 1}\right) + Z_{1S} \tag{2}$$

2. Trailing and Leading Edge Openings

In order to obtain a more regularly shaped oval domain, the second conformal mapping function of the type (11)

$$Z_3 = (Z_2 - Z_{2S})^{1/(2-\Delta\tau/\pi)} \tag{3}$$

is applied so that the leading and trailing edge regions open up into smooth curves (Figs. 4 and 5). Here $\Delta\tau$ represents the trailing edge enclosed angle. Equation (3) is also analytically invertible:

$$Z_2 = Z_{2S} + Z_3^{(2-\Delta\tau/\pi)} \tag{4}$$

If the airfoil has an open trailing edge, Z_{2S} is chosen as the mid-point between the upper and lower geometric trailing edge points. When the trailing edge is rounded, Z_{2S} becomes the point midway between the trailing edge center of curvature and the trailing edge point. The branch cut for this mapping is a straight line directed radially outward from Z_{2S} as shown in Fig. 3.

The above function (3) is applied again at the leading edge with $\Delta\tau$ and Z_{2S} determined as it was done for the trailing edge.

3. Bilinear Transformation

While opening the leading and trailing edges, the location of the physical infinities also changed. In order to preposition the domain so that the infinities are symmetrically located with respect to the center of gravity of the oval, the bilinear transformation

$$Z_5 = C\left[\frac{Z_4/R_{AV} - A}{Z_4/R_{AV} - B}\right] \tag{5}$$

is used, where the constraints A, B and C can be explicitly determined (3,12), and R_{AV} is the average radius of the oval in the Z_4-plane, such that Z_4/R_{AV} becomes an oval shape with average radius of unity. This bilinear mapping positions the upstream and downstream infinities at required locations while mapping a unit circle to a unit circle (Fig. 6). The bilinear mapping function is also analytically invertible.

4. Polar Coordinate Transformation

The oval shaped region in the $Z_5 = X_5 + iY_5$ plane is opened up into a strip (Fig. 7) of length 2π using polar coordinates

$$X_6 = \arg(Z_5) \tag{6}$$

$$Y_6 = |Z_5| \tag{7}$$

This orthogonal coordinate transformation is also analytically invertible.

5. Coordinate Shearing and Interior Grid Generation

With the increase in magnitude of the stagger angle, $|\beta|$, the images of the airfoil contour and the flow-field boundaries in the Z_6 plane will move away from the $(0,2\Pi)$ range (Fig. 7). The double images of downstream infinity, (X_6^P, Y_6^P) and $(X_6^P + 2\Pi, Y_6^P)$, are connected with the images of the double-valued trailing edge point (X_6^{TE}, Y_6^{TE}) with a simple function of a general form

$$X_6^w = X_6^P + Y^*(X_6^{TE} - X_6^P) - A' \sin(2\Pi Y^*) \qquad (8)$$

where

$$Y^* = \frac{Y_6 - Y_6^P}{Y_6^{TE} - Y_6^P} \qquad (9)$$

Here, superscript w designates wake and A' is a small input parameter. The interior grid lines of the two families are then linearly interpolated (Fig. 8). The grid thus created is re-mapped to the physical Z_1 plane by applying the inverse of each mapping function. The resulting computational grids are shown in Figures 9 - 13. Each two-dimensional grid required less than one CPU second to generate. The generation of three-dimensional grids required less than five seconds of CPU time on the CDC Cyber 170/750.

CONCLUSIONS

A three-dimensional grid generation code has been developed that is based on a sequence of conformal mappings and nonorthogonal coordinate stretching and shearing. All the mapping functions are analytically invertible thus making the technique very fast. O-type computational grids can be efficiently generated for realistically shaped axial turbines and compressors. The technique is particularly applicable to very thick, closely spaced, and highly cambered and staggered turbine blades.

ACKNOWLEDGEMENTS

This work has been supported by the Department of Aerospace Engineering and Engineering Mechanics, University of Texas at Austin. The authors are especially thankful to Ms. Patricia Diaz for typing the original and the final versions of this paper.

REFERENCES

1. Jou, Wen-Huei, "An Experience in Mesh Generation for Three-Dimensional Calculation of Potential Flow Around a Rotating Propeller," in Numerical Grid Generation, Joe F. Thompson, ed., North-Holland, 1982, pp. 547-561.

2. Thompson, Joe F., "Elliptic Grid Generation," in Numerical Grid Generation, Joe F. Thompson, ed., North-Holland, 1982, pp. 79-105.

3. Ives, D. and Liutermoza, J., "Analysis of Transonic Cascade Flow Using Conformal Mapping and Relaxation Techniques," AIAA Paper No. 76-370, AIAA 9th Fluid and Plasma Dynamics Conference, San Diego, California, July 14-16, 1976.

4. Dulikravich, D. S., "Numerical Calculation of Inviscid Transonic Flow Through Rotors and Fans," Ph.D. Thesis, Cornell University, January 1979.

5. Theodorsen, T. and Garrick, I. E., "General Potential Theory of Arbitrary Wing Sections," NACA TR 452, 1933.

6. Dulikravich, D. S., "GRID3O-Computer Program for Fast Generation of Multilevel, Three-Dimensional, O-type Boundary Conforming Computational Grids," TP 1920, 1981.

7. Dulikravich, D. S., "GRID3C-Computer Program for Generation of C-Type Multilevel Three-Dimensional, Boundary-Conforming Periodic Grids," NASA CR 167846, 1982.

8. Dulikravich, D. S., "Fast Generation of Three-Dimensional Computational Boundary-Conforming Periodic Grids of C-Type," in Numerical Grid Generation, Joe F. Thompson, ed., North-Holland, 1982, pp. 563-584.

9. Rae, W. J., "Modifications of the Ives-Liutermoza Conformal-Mapping Procedure for Turbomachinery Cascades," to be presented at the 28th ASME International Gas Turbine Conference, Phoenix, Arizona, March 27-31, 1983.

10. Traupel, W., "Die Berechnung der Strömung durch Schaufelgitter," Sul zer Techn. Rundschau Nr. 1, 1945, pp. 25-42.

11. Scholz, N., "Aerodynamics of Cascades," AGARDograph No. 220 (translated by A. Klein), 1977, pp. 261-262.

12. Mokry, M., "Comment on Analysis of Transonic Cascade Flow Using Conformal Mapping and Relaxation Techniques," AIAA Journal, Vol. 16, No. 1, January 1978, p. 96.

13. Hobson, D. E., "Shock-Free Transonic Flow in Turbomachinery Cascades," University of Cambridge, Department of Engineering, 1974.

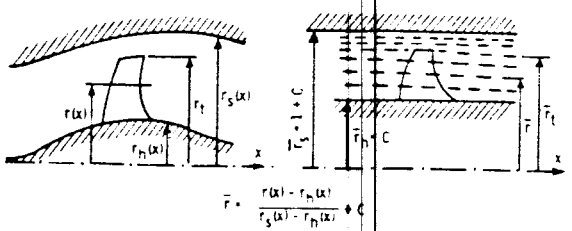

Fig. 1 Radial Coordinate Normalization in the Physical z_1 Three-Dimensional Space.

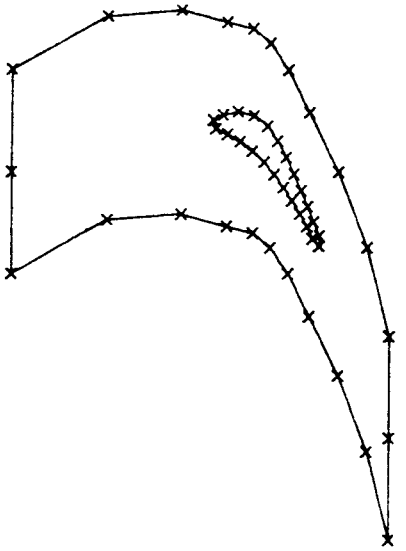

Fig. 2 Physical Plane

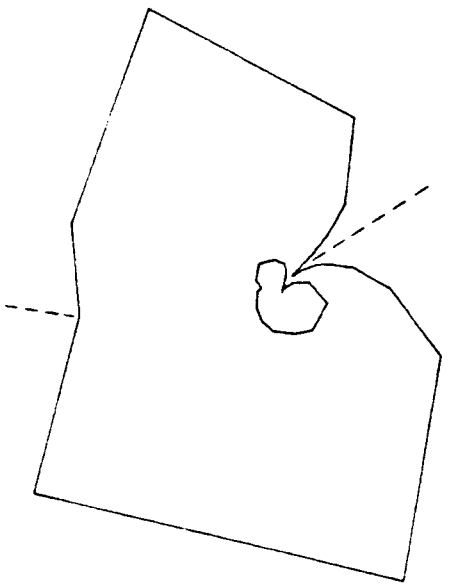

Fig. 3 Z2-Plane

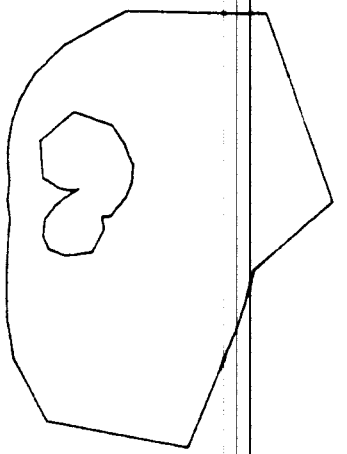

Fig. 4 Z3-Plane Showing Effect of Trailing Edge Opening

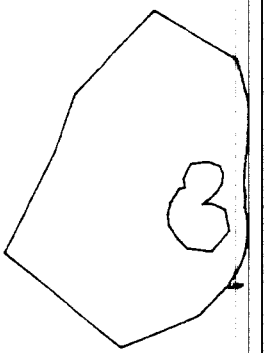

Fig. 5 Z4-Plane Showing Effect of Leading Edge Opening

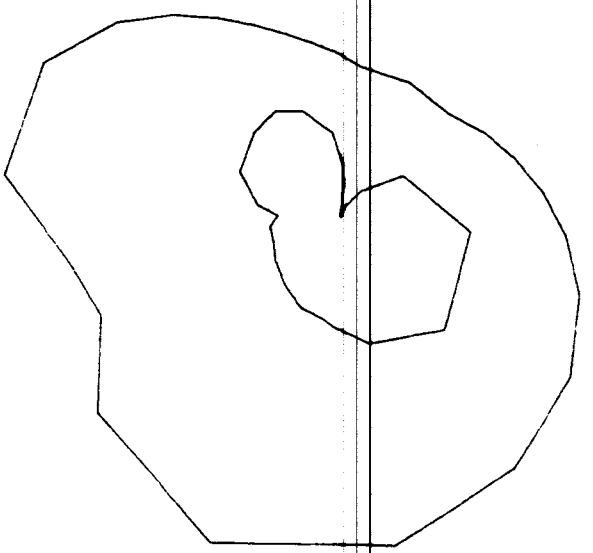

Fig. 6 Z5-Plane ("Circle" Plane)

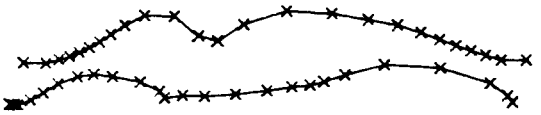

Fig. 7 Z6-Plane

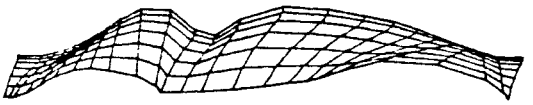

Fig. 8 Strip Plane Showing Interior Grid Generation

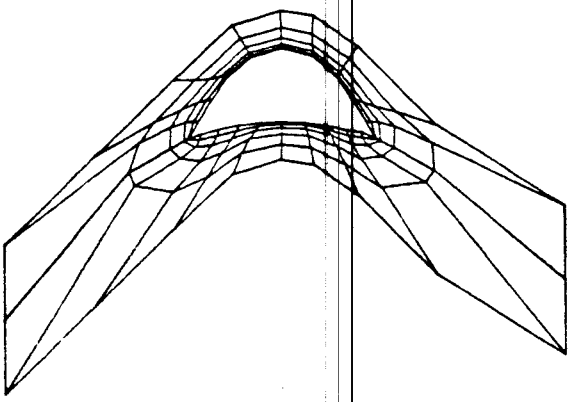

Fig. 10 Hobson's First Impulse Blade (13)
$\beta = 0.0$ Gap-to-Chord Ratio = 0.8

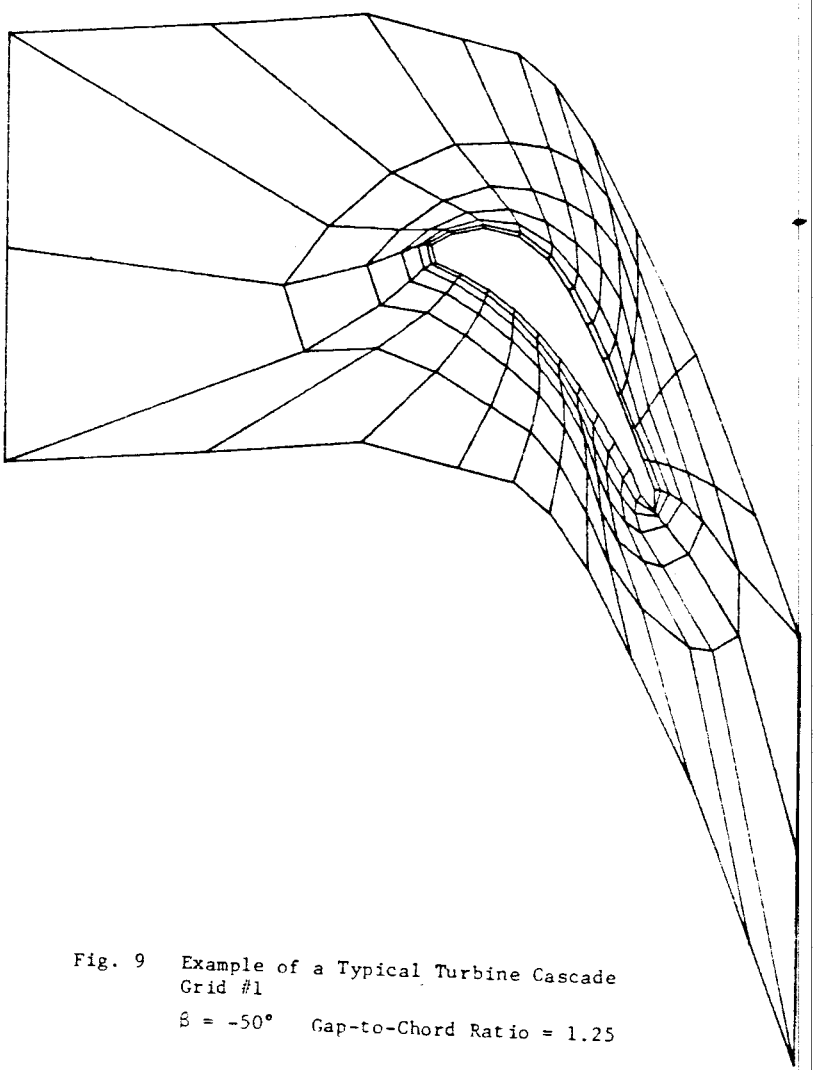

Fig. 9 Example of a Typical Turbine Cascade Grid #1
$\beta = -50°$ Gap-to-Chord Ratio = 1.25

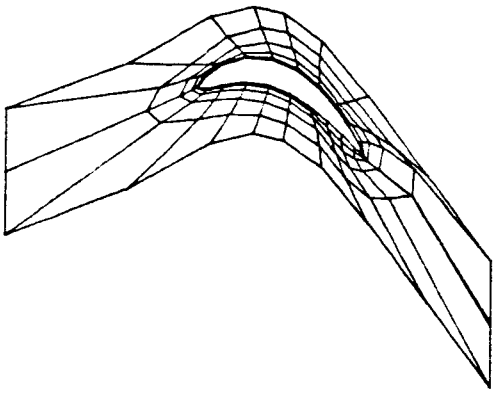

Fig. 11 Example of a Typical Turbine Cascade Grid #2

$\beta = -22.1°$ Gap-to-Chord Ratio = 0.72

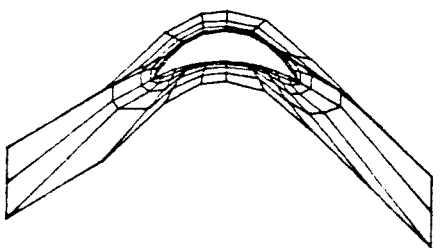

Fig. 12 Hobson's Second Impulse Blade (13)

$\beta = 0.0$ Gap-to-Chord Ratio = 0.5

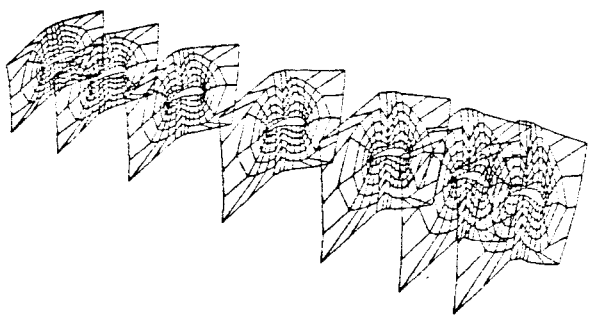

Fig. 13 Three-Dimensional Grid for a 40-Blade Turbine Rotor